Chinese Journal of Chemical Engineering 87 (2025) 197–203

Contents lists available at ScienceDirect

Chinese Journal of Chemical Engineering

journal homepage: www.elsevier.com/locate/CJChE

Full Length Article

Thermal decomposition behavior and kinetics of magnesite under carbon dioxide atmosphere

Ze Gong [1], Dexi Wang [1,*], Xueyi Ma [1], Lihua Fan [2]

[1] School of Mechanical Engineering, Shenyang University of Technology, Shenyang 110870, China
[2] School of Chemical Equipment, Shenyang University of Technology, Liaoyang 111000, China

ARTICLE INFO

Article history:
Received 20 February 2025
Received in revised form
26 July 2025
Accepted 27 July 2025
Available online 19 August 2025

Keywords:
Carbon dioxide
Reaction kinetics
Magnesite
Pyrolysis
Thermogravimetry

ABSTRACT

Using thermogravimetric experiments, the kinetic characteristics of magnesite thermal decomposition were investigated under the condition of 10% (vol) CO_2 in the actual production atmosphere of an entrained-flow dynamic roasting furnace. Based on a multi - method collaborative framework, the three kinetic factors in the magnesite thermal decomposition process were systematically calculated through parameter cross - verification between the Hu - Gao - Zhang integral method and the Kissinger differential method. The kinetic mechanism was initially screened by the double equal and double step method and further determined by combining with the Malek maximum probability method. The study revealed that CO_2 in the atmosphere exerts an inhibitory effect on the decomposition of carbonate species within magnesite. Furthermore, the presence of impurities (*e.g.*, calcium carbonate) was found to interfere with the determination of reaction mechanisms via Malek's method at elevated temperatures. The results show that in a 10% (vol) CO_2 atmosphere, the main decomposition temperature of magnesite ranges from 550°C to 650 °C, the average activation energy is 66.00 kJ·mol^{-1}, the pre-exponential factor is 1.05×10^5 s^{-1}, and the decomposition process conforms to the random nucleation and growth model.

1. Introduction

China possesses abundant magnesite reserves, with the resources highly concentrated in Liaoning and Shandong provinces [1]. Light-burned magnesia (MgO) produced from magnesite calcination serves as a crucial raw material in metallurgy, chemical engineering, refractory materials, and construction industries. Calcination, as the initial processing step, plays a pivotal role in downstream applications, making the optimization of its technology and equipment essential for sustainable industrial development [2]. In recent years, driven by environmental policies and resource integration, the industry has undergone significant technological transformation. Traditional high-energy-consumption and high-pollution shaft kilns are being phased out, while fluidized dynamic calcination furnaces—characterized by 40% lower energy consumption, broad raw material adaptability, and high product qualification rates—have emerged as the core direction for cleaner refractory production upgrades. However, current furnace designs predominantly rely on empirical experience and limited data, lacking sufficient theoretical support regarding heat transfer mechanisms, decomposition behavior, and structural influences within the reactor [3]. Therefore, in-depth research on the thermal decomposition process and kinetic characteristics of magnesite in such furnaces holds significant scientific importance for optimizing calciner design and enhancing resource utilization efficiency.

The combined thermogravimetric analysis and differential scanning calorimetry (TG-DSC) technique is a widely employed approach for investigating thermal decomposition behaviors, reaction kinetics, and phase transitions in various materials. In studies focusing on carbonate decomposition, TG-DSC analysis has revealed distinct mass loss stages associated with pyrolysis and dehydration processes. Furthermore, this technique has proven effective in quantitatively assessing the influence of heating rates and particle size on the decomposition kinetics of carbonates [4,5]. Regarding the decomposition mechanism of magnesite, multiple reaction models have been proposed. Bai *et al.* [6] suggested that magnesite decomposition follows a three-dimensional phase boundary reaction-controlled mechanism, whereas Liu *et al.* [7] argued that the process is governed by three-dimensional diffusion control. Reported activation energy values for magnesite decomposition in inert or air atmospheres vary considerably

* Corresponding author.
E-mail address: wangdexi@sut.edu.cn (D. Wang).

https://doi.org/10.1016/j.cjche.2025.07.014

across literature. Mancarella *et al.* [8] investigated magnesite thermal decomposition under vacuum conditions, demonstrating that particles sized 20-50 μm began decomposing at 620 °C with an activation energy of 120 kJ·mol^{-1}. Conversely, Bai *et al.* [9] reported an activation energy of 172 kJ·mol^{-1} for 0.074 μm particles in air atmosphere. These discrepancies highlight the sensitivity of activation energy to material composition, particle size, and experimental conditions. In practical magnesite calcination processes, the decomposition occurs in an atmosphere containing substantial CO_2 from fuel combustion, which significantly influences the decomposition behavior. Studies by Ma *et al.* [10] and Subagjo *et al.* [11] revealed that the activation energy of magnesite decomposition increases with rising CO_2 concentration, while the reaction mechanism also undergoes alterations. However, these investigations failed to account for the actual CO_2 concentration levels present in industrial furnace environments, resulting in findings that deviate from real-world decomposition characteristics and cannot accurately reflect in-furnace processes.

This study addresses this research gap by systematically measuring operational parameters (including feed rate, fuel consumption, and gas intake) from a 105 kg·h^{-1} experimental setup to determine actual in-furnace CO_2 concentrations. Using thermogravimetric analysis, we investigate the thermal decomposition kinetics of magnesite under these industrially relevant conditions. The findings provide theoretical support for understanding the necessity and impact of CO_2 concentration control in the design of next-generation calcination furnaces.

2. Experimental

2.1. Materials

The experimental study employed magnesite ore from the Liaodong Peninsula, which underwent manual sorting to remove talc gangue constituents. The raw material was initially processed through jaw crusher coarse crushing to achieve particle sizes below 20 mm, followed by wet ball milling refinement to attain a median particle diameter (D_{50}) of 25 μm. The resultant particle size distribution is graphically presented in Fig. 1, with corresponding chemical composition data detailed in Table 1.

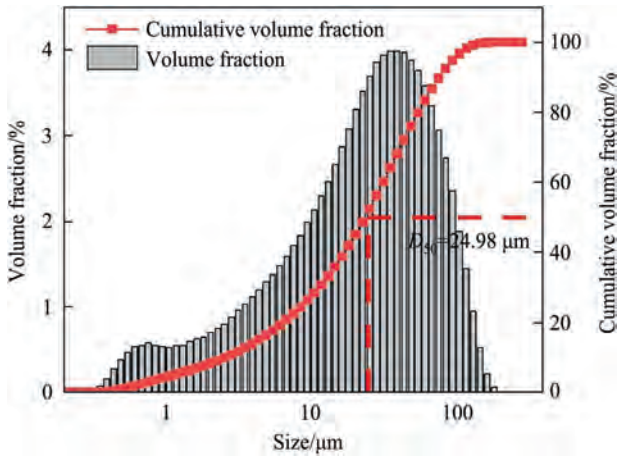

Fig. 1. Particle size distribution of magnesite sample.

Table 1
Composition of magnesite raw material.

Ingredient	MgO	SiO_2	Fe_2O_3	CaO	Loss on Ignition
Content/%(mass)	46.9	0.54	0.29	0.66	52

2.2. Determination of experimental atmosphere

Within gas-flow bed dynamic calcination furnaces, magnesite ore interacts with high-temperature flue gas, inducing rapid decomposition of magnesium carbonate and calcium carbonate constituents. Given the negligible concentrations of other mineral phases, this investigation specifically focuses on the thermal decomposition of magnesium carbonate. The decomposition reaction is expressed as:

$$MgCO_3(s) = MgO(s) + CO_2(g)\uparrow$$

The pilot-scale gas-flow bed dynamic calcination furnace demonstrates operational parameters with a feed rate of 105 kg·h^{-1} and natural gas consumption of 20 m^3·h^{-1} (normal cubic meters per hour). The fuel exhibits a calorific value of 35.99 MJ·m^{-3}, with its detailed composition provided in Table 2.

Based on the stoichiometry of the magnesium carbonate decomposition reaction and the operational feed rate, the CO_2 generation rate from the decomposition process was calculated as follows:

$$V_{CO_2} = \frac{m_{MgCO_3} Mr_{CO_2}}{Mr_{MgCO_3} \rho_{CO_2}} \quad (1)$$

The calculation formula for determining the flue gas generation volume in combustion processes is expressed as follows [12]:

$$V = V_1 \left\{ a \left[V_1 \left(\frac{0.264}{1000} Q_d + 0.02 \right) \right] + 0.38 + \left(\frac{0.018}{1000} Q_d \right) \right\} \quad (2)$$

Where V_1 is the fuel consumption, in m^3·h^{-1}; Q_d is the fuel calorific value, in kJ·m^{-3}; V is the volume of combustion flue gas generated, in m^3·m^{-3}; a is the combustion air coefficient, with a value range of 1.10 to 1.30.

By substituting operational parameters into Eqs. (1) and (2), the pilot-scale system's air consumption was determined as 190.4 m^3·h^{-1}, with combustion-generated gas volume reaching 220.5 m^3·h^{-1}. Based on the composition of natural gas and atmospheric CO_2 content, the calculated CO_2 production rates were determined to be 20.2 m^3·h^{-1} from combustion and 27.8 m^3·h^{-1} from magnesium carbonate decomposition. This results in an initial CO_2 concentration of 10%(vol) in the circulating fluidized bed dynamic calciner, which increases to 20% upon complete magnesite decomposition. Accordingly, thermogravimetric experiments were conducted under controlled atmospheres with 0%, 10%, and 20%(vol) CO_2 concentrations to simulate the flue gas composition at different operational stages of the dynamic calciner, thereby systematically investigating the influence of CO_2 concentration on decomposition kinetics.

2.3. Experimental method

The raw material pretreatment was conducted using a DHG-9070A-T drying oven, where magnesite powder was continuously dried at a constant temperature of 120 °C for 12 h to reduce free water content to ≤0.5%, thereby minimizing interference from moisture evaporation during thermogravimetric analysis. Thermal decomposition experiments were performed using a Beijing Hengjiu CHT-4 simultaneous thermal analyzer in the temperature

Table 2
Natural gas composition.

Ingredient	CH_4	C_2H_6	C_3H_8	C_4H_{10}	CO_2	O_2	N_2	C_6H_{14}
Content/%(vol)	86.31	4.15	1	0.24	1.84	0.40	6.05	0.02

range of 25–900 °C.For each experiment, 10 mg of magnesite sample was loaded into an alumina crucible and tested under three controlled atmospheres: (1) 100% (vol) N_2, (2) 10% CO_2 + 90% N_2, and (3) 20% CO_2 + 80% N_2, with a constant gas flow rate of 120 ml·min^{-1}. The samples were heated to 900 °C at five different heating rates (5, 10, 15, 20, and 25 °C·min^{-1}) to obtain TG-DSC curves under varying temperature programs. Non-isothermal kinetic analysis was performed using the Hu-Gao-Zhang integral method and Kissinger differential method to determine the activation energy (E) and pre-exponential factor (A). The kinetic mechanism was preliminarily screened through the double equal-double steps method and subsequently verified using Malek's maximum probability method to identify the most appropriate kinetic model.

3. Results and Discussion

3.1. Decomposition of magnesite

Under the aforementioned experimental conditions, the mass loss behavior of magnesite decomposition at a heating rate of 10 °C·min^{-1} was obtained for three different CO_2 concentrations, as shown in Fig. 2. The three curves exhibit nearly identical behavior in the low-temperature region, with minimal mass loss (close to 1.0), indicating that decomposition had not yet initiated or was extremely slow. As the temperature increased to 500–600 °C, all three curves displayed a sharp decline, signifying the rapid completion of the primary decomposition reaction within this temperature range. Beyond 700 °C, the mass loss process approached completion, with the curves stabilizing at a constant level, indicating that the decomposition reaction had essentially finished. A comparison of the three curves reveals that the presence of CO_2 significantly increased the decomposition temperature of magnesite. In pure N_2 atmosphere, rapid mass loss began at the lowest temperature (560–570 °C). In the 10%(vol) CO_2 atmosphere, the onset of rapid mass loss shifted to a higher temperature (590–600 °C), while in the 20%(vol) CO_2 atmosphere, the onset temperature was highest (630–640 °C). This phenomenon suggests that increasing CO_2 concentration in the gas phase inhibits the decomposition reaction by raising the equilibrium CO_2 partial pressure in the system. Consequently, a higher initial temperature is required to overcome the increased equilibrium resistance.

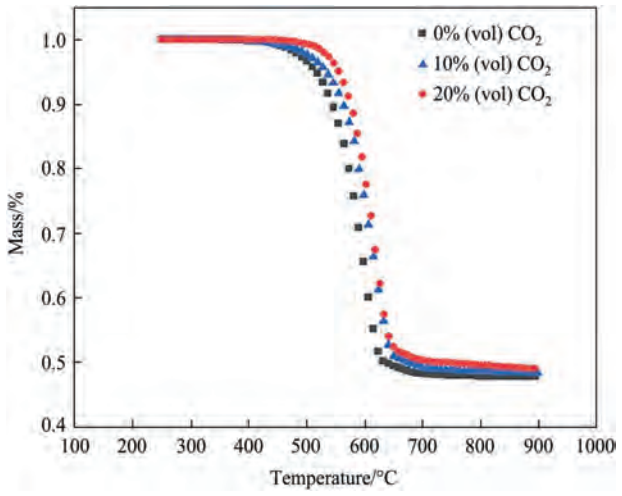

Fig. 2. The mass loss curves of magnesite decomposition under different CO_2 concentration atmospheres.

During the rapid mass loss stage, the slope of the curve under higher CO_2 concentration appears steeper than that under lower CO_2 concentration, implying that although elevated CO_2 delays the onset of decomposition, it may enhance the maximum reaction rate to some extent. Upon completion of the reaction, all three curves stabilized at a residual mass fraction of approximately 50% (mass), whereas the theoretical residual mass fraction for pure magnesite fully decomposed to MgO is 47.8%(mass). The higher measured value strongly indicates the presence of impurities in the sample. The single-step mass loss observed in all three curves suggests that the decomposition follows a one-step reaction mechanism [13].

3.2. Kinetic parameter calculation

The kinetic behavior of magnesite decomposition into magnesium oxide and CO_2 under high-temperature calcination conditions can be systematically described using non-isothermal solid-state reaction kinetics theory [14,15]. The mathematical formalism governing this process is expressed as follows:

$$\frac{d\alpha}{dt} = \left(\frac{1}{\beta}\right)k(T)f(\alpha) = \frac{A}{\beta}f(\alpha)\exp\left(-\frac{E}{RT}\right) \tag{3}$$

Where, α is the conversion rate of the magnesite decomposition process; t is the time; β is the heating rate; $K(T)$ is the temperature dependence of the rate constant (reaction rate constant); $f(\alpha)$ is the reaction mechanism function; A is the apparent pre-exponential factor; E is the activation energy.

In non-isothermal kinetic analysis systems, the selection of kinetic model functions significantly impacts the numerical precision of Arrhenius parameter solutions. When employing differential methods for computation, mathematical discrepancies in the mechanistic functions $f(\alpha)$ induce systematic deviations in calculated activation energy and pre-exponential factor. Consequently, during the determination of kinetic triplets [$f(\alpha)$, E, A], it is imperative to employ distinct computational approaches for at least one parameter to ensure methodological robustness [7]. In this study, the Hu-Gao-Zhang integral method and Kissinger differential method [16,17] were systematically applied to derive kinetic parameters for magnesite thermal decomposition.

Through integral transformation of Eq. (3) in conjunction with non-isothermal kinetic theory, the Hu-Gao-Zhang equation is derived as follows:

$$\ln\left[\frac{\beta}{T^{1.882}}\right] = \left[\ln\frac{AE}{RG(\alpha)} + 3.986 - 1.882nE\right] - 1.002\frac{E}{RT} \tag{4}$$

Based on non-isothermal kinetic analysis data obtained at heating rates of 5–20 °C·min^{-1}, Eq. (4) was applied to perform linear fitting for is conversional points at $\alpha = 0.2$–0.8, as illustrated in Fig. 3. The near-parallel slopes of the fitted lines demonstrate that the activation energy of magnesite decomposition remains essentially constant throughout the main reaction stage, confirming that the decomposition follows a single reaction mechanism [18].

Through differential derivation of Eq. (3) under non-isothermal reaction conditions, the Kissinger equation is obtained as follows:

$$\ln\left(\frac{\beta}{T^2}\right) = \ln\frac{AR}{E} - \frac{E}{RT} \tag{5}$$

When applying the Kissinger equation to calculate kinetic parameters for magnesium carbonate thermal decomposition, it is essential to acquire TG-DTG curves at varied heating rates β utilizing the peak temperatures from the mass loss inflection points

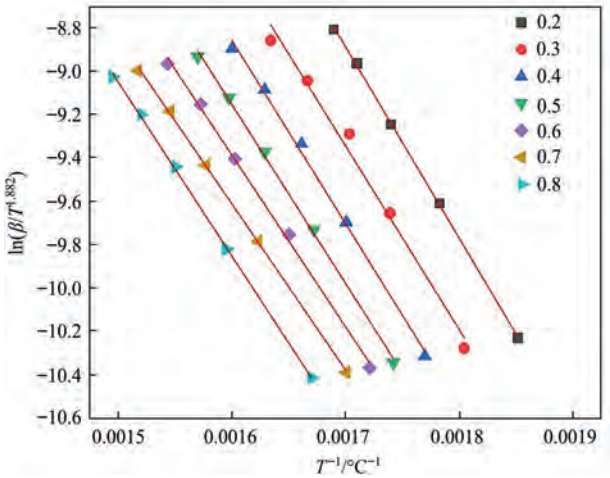

Fig. 3. The relationship between $\ln(\beta/T^{1.882})$ and $1/T$

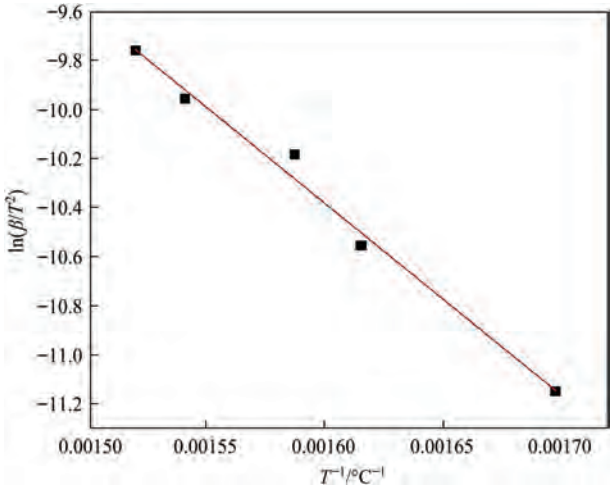

Fig. 4. Fitting relationship between $\ln(\beta/T^2)$ and $1/T$ in the calcination of magnesite powder.

of each curve, the activation energy E and pre-exponential factor A can be determined through the linear correlation between $\ln(\beta/T^2)$ and $1/T$, as illustrated in Fig. 4.

The activation energies and pre-exponential factors derived from experimental data through the Hu-Gao-Zhang equation and Kissinger equation are summarized in Table 3. These kinetic parameters serve to quantitatively characterize the decomposition behavior of magnesium carbonate, providing critical foundational data for subsequent model construction and reaction mechanism analysis. Notably, the Hu-Gao-Zhang equation, grounded in integral methodology, demonstrates broad applicability across diverse experimental conditions, while the Kissinger equation facilitates rapid estimation *via* differential approaches. Comparative analysis of computational results from these two methods further validates experimental reliability through methodological cross-verification.

Table 3
Kinetic parameters of magnesite thermal decomposition.

Method	E/kJ·mol^{-1}	ln$A$/s^{-1}	r^2
Hu-Gao-Zhang equation	67.19	12.06	>0.988
Kissinger equation	64.82	11.05	0.989
Average	66.00	11.56	

Table 4
Basic data of fitting curves for Assumed mechanism functions.

Mechanism	$G(\alpha)$	$-k$	r^2
R2	$1-(1-\alpha)^{1/2}$	0.9426	0.9987
R3	$1-(1-\alpha)^{1/3}$	0.9668	0.9987
A1	$-\ln(1-\alpha)$	1.0169	0.9985
A2	$[-\ln(1-\alpha)]^{1/2}$	0.5083	0.9985
A3	$[-\ln(1-\alpha)]^{1/3}$	0.3389	0.9992
D2	$\alpha+(1-\alpha)\ln(1-\alpha)$	0.3829	0.9986
D3	$\left[1-(1-\alpha)^{1/3}\right]^2$	1.9335	0.9987
D4	$1-\frac{2}{3}\alpha-(1-\alpha)^{2/3}$	1.8685	0.9987

3.3. Determination of the reaction mechanism function

This study employed a dual equal-step methodological approach to ascertain the reaction mechanism function governing magnesite decomposition [19]. Through phase-shift transformation of the Flynn-Wall-Ozawa equation, the derived functional relationship expressed as Eq. (6) was systematically established.

$$\lg G(\alpha)=\left[\lg\left(\frac{AE}{R}\right)-2.314-0.4567\frac{E}{RT}\right]-\lg\beta \tag{6}$$

Given that magnesite decomposition adheres to a single-step reaction mechanism, the dual equal-step method allows for mechanistic function determination through analysis at any selected temperature during the reaction process. By incorporating the α values (0.1–0.9) from thermogravimetric (TG) curves within the isothermal nodal range of 550–750 °C, the predefined mechanism function $G(\alpha)$, and heating rates β = 5–25 °C·min^{-1} into Eq. (6), linear regression analysis was performed to derive the correlation coefficient r^2 and slope k of the fitted linear profiles. The computational results across varying temperatures are systematically tabulated in Table 4.

Based on the results presented in Table 4, the slopes of the predefined mechanism functions R2, R3, and A1 all approximate −1 with high correlation coefficients, suggesting that further determination of the mechanism function governing magnesite decomposition remains necessary. To minimize experimental uncertainties, the effective reaction interval of conversion rate $\alpha \in [0.1,0.9]$ was selected. By identifying characteristic temperature points within this range and applying consistent computational methodology, the slopes and correlation coefficients corresponding to mechanism functions R2, R3, and A1 were recalculated. These refined results are systematically summarized in Table 5.

Table 5
Basic data of fitting curves for three mechanism functions.

Temperature/°C	Function	$-k$	r^2
576	R2	0.9426	0.9987
	R3	0.9825	0.9996
	A1	1.0547	0.9987
588	R2	0.9839	0.9983
	R3	1.0471	0.9988
	A1	1.1463	0.9957
600	R2	1.0156	0.9983
	R3	1.0885	0.9957
	A1	1.2496	0.9914

The results demonstrate that at lower temperatures, the A1 mechanism function (random nucleation) yields fitted linear slopes demonstrating close proximity to −1 with high correlation coefficients r^2, whereas at elevated temperatures, the slope k of the fitted straight line for the R2 mechanism function also approaches −1, exhibiting a high correlation coefficient r^2. Consequently, through joint validation of both model goodness-of-fit and activation energy matching degree, the thermal decomposition kinetics of magnesite are preferentially governed by dual control mechanisms: A1 (stochastic nucleation) and R2 (interfacial reaction). Given the convergence of multivariate linear fitting accuracies, this study implements Malek's method for kinetic analysis in thermal analysis to resolve the reaction mechanism. By constructing the α-conversion function $y(\alpha)$, the dominant mechanism function governing magnesite decomposition is conclusively identified.

Based on the reaction rate equation and Coats-Redfern method, the following kinetic equation can be derived:

$$G(\alpha)=\frac{RT^2}{E\beta}\frac{\mathrm{d}\alpha}{\mathrm{d}t}\frac{1}{f(\alpha)} \tag{7}$$

At $\alpha = 0.5$, there is Eq. (11).

$$G(0.5)=\frac{RT_{0.5}^2}{E\beta}\left(\frac{\mathrm{d}\alpha}{\mathrm{d}t}\right)_{0.5}\frac{1}{f(0.5)} \tag{8}$$

In the equation, $T_{0.5}$ is the temperature at $\alpha = 0.5$; $k_{0.5}$ is the reaction rate at $\alpha = 0.5$.

Dividing Eq. (7) by Eq. (8) yields the annotated curve Eq. (9).

$$y(\alpha)=\left(\frac{T}{T_{0.5}}\right)^2\frac{\left(\frac{\mathrm{d}\alpha}{\mathrm{d}t}\right)}{\left(\frac{\mathrm{d}\alpha}{\mathrm{d}t}\right)_{0.5}}=\frac{f(\alpha)G(\alpha)}{f(0.5)G(0.5)} \tag{9}$$

By substituting the experimental data corresponding to each time point into Eq. (9), the α-dependent curve of the experimental dataset can be generated. The most probable mechanism function can be determined by comparing the degree of agreement between the experimental curve and standard theoretical curves. Taking a constant heating rate of 10 °C·min^{-1} as an example, the resulting $y(\alpha)$-α functional relationship is illustrated in Fig. 5.

As indicated by experimental curve e in Fig. 5, the trajectory closely aligns with the standard curve of reaction mechanism A1 at low conversion rates (α < 0.8), demonstrating high kinetic correlation in this regime. With increasing α, the experimental curve deviates from A1, and the best-fitting standard curves sequentially shift to R2 and R3. This deviation originates from $CaCO_3$ impurities in the sample: The significant disparity in ionic radii between Ca^{2+} and Mg^{2+} induces localized strain, lattice defects, or heterogeneous interfaces upon $CaCO_3$ incorporation into magnesite. These microstructural alterations function as either catalytic nuclei or diffusion barrier, thereby modifying local reaction kinetics and causing deviations from the expected behavior predicted by pure magnesite models. Critically, the decomposition temperature of $CaCO_3$ exceeds that of $MgCO_3$ in magnesite. Thus, during magnesite decomposition, $CaCO_3$ remains thermally stable. Upon further heating into the $CaCO_3$ decomposition range—where magnesite has fully decomposed—the onset of calcite breakdown generates a secondary decomposition peak in the experimental curve at α > 0.95. This phase transition results in further divergence from the original standard curves. Therefore, the dominant decomposition mechanism for magnesite is identified as A1.

This study adopts the mechanism function corresponding to the A1 (random nucleation) model as the presumptive kinetic formalism. Under identical heating rates, discrete conversion values α and their corresponding temperatures were systematically incorporated into the Coats-Redfern equation [20] for computational analysis. Linearization processing of thermogravimetric data yielded the fitted regression lines illustrated in Fig. 6. Kinetic deconvolution reveals an apparent activation energy of 77.16 kJ·mol^{-1} for the magnesite decomposition process, demonstrating significant convergence with computational outcomes derived from both the Hu-Gao-Zhang method and Kissinger's differential technique. This methodological corroboration validates the reliability of multi-method coupling strategies in activation energy determination.

Comprehensive kinetic analysis has verified that the thermal decomposition process of magnesite conforms to the A1 reaction mechanism. The integral form of its reaction mechanism function is $G(\alpha) = -\ln(1-\alpha)$, and the differential form is $f(\alpha) = 1-\alpha$.

The activation energies, pre-exponential factors, and mechanism functions for magnesite decomposition in N_2 atmosphere and 20%(vol) CO_2 + 80%(vol) N_2 atmosphere were determined following the methodology described above. The results are presented in Table 6.

As can be seen from Table 6, the kinetic parameters of magnesite decomposition vary with the CO_2 concentration in the

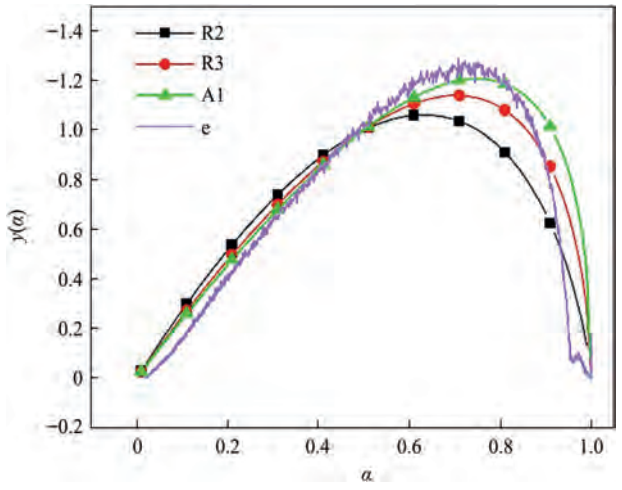

Fig. 5. Standard $y(\alpha)$-α relationship curve and experimental $y(\alpha)$-α relationship curve.

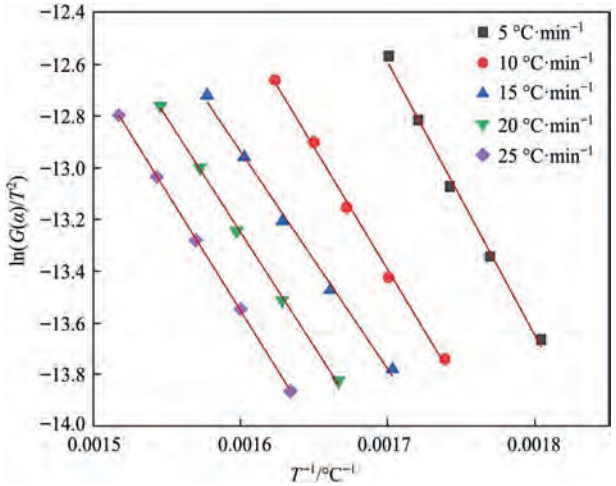

Fig. 6. Fitting relationship between $\ln(G(\alpha)/T^2)$ and $1/T$ in the calcination of magnesite powder.

Table 6
Kinetic parameters for magnesite decomposition under varying CO_2 atmospheres.

Atmosphere	E/kJ·mol^{-1}	G(α)	A/s^{-1}
N_2	60	$G(\alpha) = -\ln(1-\alpha)$	2.35×10^5
10%CO_2+90%N_2	66	$G(\alpha) = -\ln(1-\alpha)$	1.05×10^5
20%CO_2+80%N_2	89	$G(\alpha) = -\ln(1-\alpha)$	6.7×10^4

decomposition atmosphere. As the CO_2 concentration increases, the activation energy rises while the pre-exponential factor decreases. This occurs because CO_2, as a decomposition product, enhances the reverse reaction when its concentration increases and adsorbs onto active sites, thereby raising the energy barrier for decomposition and increasing the activation energy. High CO_2 concentrations also hinder the diffusion of decomposition products, leading to a reduction in the pre-exponential factor.

3.4. Influence of water vapor in flue gas on the reaction

The calcination of magnesite using natural gas as fuel inevitably produces water vapor during the combustion reaction. Theoretical calculations indicate that the water vapor concentration in the flue gas remains consistently maintained at approximately 18% (vol). Current research demonstrates that below 400 °C, magnesite composition rates remain minimal in both dry and steam-containing atmospheres, with negligible water vapor influence. However, at elevated temperatures of 500 °C, flue gas moisture significantly enhances decomposition kinetics [21]. Four mechanistic pathways have been proposed to explain this catalytic effect: (1) reduction of gas diffusion resistance during calcination, thereby accelerating reaction kinetics [22]; (2) adsorption on nascent MgO active sites, which weakens CO_2-MgO binding energy and mitigates product inhibition [23,24]; (3) formation of deep pore structures that expand reactive interfaces and facilitate CO_2 desorption; and (4) enhanced thermal conductivity that improves material heating rates [21]. These findings collectively establish the pronounced promotional effect of flue gas-derived water vapor on magnesite decomposition.

The dynamic variations of CO_2 concentration in industrial furnaces require further investigation from both spatial and temporal perspectives. Future research should focus on regulating flue gas moisture gradients and elucidating the spatiotemporal distribution characteristics of CO_2 within industrial furnaces. Future investigations should prioritize precise control of moisture gradients and characterization of spatiotemporal CO_2 distribution patterns in industrial kilns.

4. Conclusions

This study employed thermogravimetric analysis to confirm that CO_2 significantly inhibits the thermal decomposition kinetics of magnesite under simulated calcination atmospheres. This inhibition manifests as a regular increase in both the initial and peak decomposition temperatures with rising CO_2 partial pressure, accompanied by a reduction in reaction rate. To precisely characterize the kinetic parameters under this inhibitory effect, a synergistic approach was adopted, combining the isoconversional method (Hu-Gao-Zhang) and the variable heating rate method (Kissinger). Under a 10% (vol) CO_2 atmosphere, joint calculations determined the apparent activation energy for magnesite decomposition to be 66.0 kJ·mol^{-1} and the pre-exponential factor to be 1.05×10^5 s^{-1}. This combined methodology effectively enhanced the reliability of the determined parameters. Through cross-validation using the double parallel-step method and Malek's maximum probability method, the most probable mechanism function for decomposition under these conditions was identified as having the integral form $G(\alpha) = -\ln(1-\alpha)$ and the differential form $f(\alpha) = 1-\alpha$, revealing the specific decomposition pathway. The study also indicates that water vapor potentially present in the atmosphere may exert a promoting effect. This promotion forms complex coupling effects with the CO_2 inhibition, the detailed mechanism of which requires further investigation. The core kinetic parameters and mechanism models established herein provide crucial theoretical support for analyzing the 'atmosphere-reaction' coupling interactions within industrial kilns and for advancing the development of energy-efficient and low-carbon magnesite calcination technologies.

CRediT Authorship Contribution Statement

Ze Gong: Writing – original draft. Dexi Wang: Writing – review & editing. Xueyi Ma: Funding acquisition. Lihua Fan: Writing – Project administration.

Declaration of Competing Interest

The authors declare that they have no known competing financial interests or personal relationships that could have appeared to influence the work reported in this paper.

Acknowledgements

This research was supported by the Natural Science Foundation of Liaoning Province (2024-MSLH-360).

References

[1] Y. Han, S. Wu, Y. Han, K.M. Zhao, Y.B. Li, B.Z. Yang, M.C. Sun, H. Wang, A new round of high-quality development countermeasures for Liaoning magnesite industry, *Mod. Ind. Econ. Informationization* 14 (4) (2024) 26–28.
[2] F. Gao, L.L. Fu, D.R. Bai, G.W. Xu, Study on the thermal decomposition reaction behavior and kinetic characteristics of millimeter sized magnesite particles in fluidization, *Chin. J. Process Eng.* 23 (10) (2023) 1435–1445.
[3] J.L. Zhang, L. Zhao, H. Dong, D.X. Wang, Study on the thermal process and calcination gas flow rate of light-burned magnesia entrained-flow calciner, *Inorg. Chem. Ind.* 54 (1) (2022) 96–100.
[4] R.H. Lu, Comparison of the decomposition characteristics and kinetics of magnesite with limestone under high temperature suspension state, *Cem. Eng.* (2) (2018) 13–16.
[5] F. Demir, B. Dönmez, H. Okur, F. Sevim, Calcination kinetic of magnesite from thermogravimetric data, *Chem. Eng. Res. Des.* 81 (6) (2003) 618–622.
[6] L.M. Bai, Y.F. Deng, X.X. Li, Y.X. Ma, Z.B. Xing, Research on decomposition kinetics of fine grained magnesite, *Non Met. Mines* 39 (5) (2016) 7–9.
[7] X.W. Liu, Y.L. Feng, H.R. Li, P. Zhang, P. Wang, Thermal decomposition kinetics of magnesite from thermogravimetric data, *J. Therm. Anal. Calorim.* 107 (1) (2012) 407–412.
[8] F. Mancarella, M. D'Elia, G. Micca Longo, S. Longo, V. Orofino, Kinetics of thermal decomposition of particulate samples of $MgCO_3$: experiments and models, *Chemistry* 4 (2) (2022) 548–559.
[9] L.M. Bai, Y.F. Deng, Y.X. Han, W.Q. Zhao, Thermal decomposition process and kinetics of microfine magnesite, *J. Northeast. Univ. Nat. Sci.* 39 (3) (2018) 398–403.
[10] X.Y. Ma, B. Liu, G. Chen, L.H. Fan, D.X. Wang, The kinetic mechanism of magnesite thermal decomposition under N_2 and CO_2 atmospheres, *Chin. J. Process Eng.* 24 (8) (2024) 946–954.
[11] S. Subagjo, W. Wulandari, P.M. Adinata, A. Fajrin, Thermal decomposition of dolomite under CO_2-air atmosphere, *AIP Conf. Proc.* 1805 (2017) 040006.
[12] B.Q. Wang, Industrial Furnace Design Manual, China Machine Press, Beijing, 2010. (in Chinese)
[13] L.L. Xu, N.R. Yang, H.L. Tao, Y.H. Yin, Effect of chemical activity of MgO on cracking and water-resistance of magnesium oxychloride materials, *J. Chin. Ceram. Soc.* 31 (8) (2003) 759–762, 769.
[14] G. Kaur, S. Kainth, R. Kumar, P. Sharma, O.P. Pandey, Reaction kinetics during non-isothermal solid-state synthesis of boron trioxide *via* boric acid dehydration, *React. Kinet. Mech. Catal.* 134 (1) (2021) 347–359.
[15] S.L. Niu, K.H. Han, C.M. Lu, R.Y. Sun, Thermogravimetric analysis of the relationship among calcium magnesium acetate, calcium acetate and magnesium acetate, *Appl. Energy* 87 (7) (2010) 2237–2242.

[16] S. Vyazovkin, Kissinger method in kinetics of materials: things to beware and be aware of, *Molecules* 25 (12) (2020) 2813.
[17] H.E. Kissinger, Reaction kinetics in differential thermal analysis, *Anal. Chem.* 29 (11) (1957) 1702−1706.
[18] X.W. Liu, Y.L. Feng, H.R. Li, Preparation of basic magnesium carbonate and its thermal decomposition kinetics in air, *J. Cent. South Univ. Technol.* 18 (6) (2011) 1865−1870.
[19] L.S. Thakur, A.K. Varma, P. Mondal, Analysis of thermal behavior and pyrolytic characteristics of vetiver grass after phytoremediation through thermogravimetric analysis, *J. Therm. Anal. Calorim.* 131 (3) (2018) 3053−3064.
[20] A.W. Coats, J.P. Redfern, Kinetic parameters from thermogravimetric data, *Nature* 201 (4914) (1964) 68−69.
[21] H. Ababneh, A.P. Chen, B. Dally, Steam calcination of magnesite for the production of reactive magnesia, Miner. Process. Extr. Metall. Rev. 1−14.
[22] J. Fagerlund, J. Highfield, R. Zevenhoven, Kinetics studies on wet and dry gas−solid carbonation of MgO and $Mg(OH)_2$ for CO_2 sequestration, *RSC Adv.* 2 (27) (2012) 10380−10393.
[23] N. Rong, J.H. Wang, K.W. Liu, L. Han, Z.Y. Mu, X. Liao, W.J. Meng, Enhanced CO_2 capture durability and mechanical properties using cellulose-templated CaO-based pellets with steam injection during calcination, *Ind. Eng. Chem. Res.* 62 (3) (2023) 1533−1541.
[24] N. Rong, Q.H. Wang, M.X. Fang, L.M. Cheng, Z.Y. Luo, K.F. Cen, Steam hydration reactivation of CaO-based sorbent in cyclic carbonation/calcination for CO_2 capture, *Energy Fuels* 27 (9) (2013) 5332−5340.